## Can Ferroelectricity Improve Organic Solar Cells?

Abdu-Aguye, Mustapha; Doumon, Nutifafa Y.; Terzic, Ivan; Dong, Jingjin; Portale, Giuseppe; Loos, Katja; Koster, L. Jan Anton; Loi, Maria Antonietta

# Can Ferroelectricity Improve Organic Solar Cells?

*Mustapha Abdu-Aguye, Nutifafa Y. Doumon, Ivan Terzic, Jingjin Dong, Giuseppe Portale, Katja Loos, L. Jan Anton Koster,\* and Maria Antonietta Loi\**

Blends of semiconducting (SC) and ferroelectric (FE) polymers have been proposed for applications in resistive memories and organic photovoltaics (OPV). For OPV, the rationale is that the local electric field associated with the dipoles in a blend could aid exciton dissociation, thus improving power conversion efficiency. However, FE polymers either require solvents or processing steps that are incompatible with those required for SC polymers. To overcome this limitation, SC (poly(3-hexylthiophene)) and FE (poly(vinylidene fluoride-trifluoroethylene)) components are incorporated into a block copolymer and thus a path to a facile fabrication of smooth thin films from suitably chosen solvents is achieved. In this work, the photophysical properties and device performance of organic solar cells containing the aforementioned block copolymer consisting of poly(vinylidene fluoride-trifluoroethylene): P(VDF-TrFE), poly(3-hexylthiophene): P3HT and the electron acceptor phenyl-$C_{61}$-butyric acid methyl ester: [60]PCBM are explored. A decrease in photovoltaic performance is observed in blends of the copolymer with P3HT:[60]PCBM, which is attributed to a less favorable nanomorphology upon addition of the copolymer. The role of lithium fluoride (the cathode modification layer) is also clarified in devices containing the copolymer, and it is demonstrated that ferroelectric compensation prevents the ferroelectricity of the copolymer from improving photovoltaic performance in SC-FE blends.

Blends of semiconducting donor polymers (D) and fullerene derivatives as acceptors (A) have been studied over the past two decades as the highest performing configuration for organic photovoltaics. At the same time, other materials with different functionalities have been explored as useful additives to these D-A blends such as other polymers or small molecules[1–3] as in ternary blends; or metal (chalcogenide) nanoparticles as in hybrid blends in which the absorption of the added material is meant

to augment that of the D-A blend,[4–7] to aid with transport (as an additional D or A) or as a compatibilizer to improve morphology.[8–10] Recently, a few groups reported the use of ferroelectric (FE) polymers such as poly(vinylidene difluoride)– PVDF and poly(vinylidene difluoride trifluoroethylene)–P(VDF-TrFE) as additives to organic solar cells citing the presence of electric dipoles, which give rise to the FE properties, as the main cause of the observed enhancement in power conversion efficiency (PCE).[11,12] Afterward, Braz et al. published another study on the photophysics of a family of polyfluorene-based polymers, opining that the local electric field, created by the ferroelectric polymer induces a photoluminescence quenching, translated into a reduction of both photoluminescence intensity and lifetime.[13] The idea behind all these was that the presence of dipoles would have a favorable effect on the dissociation of excitons formed in the semiconducting part of the blend. Since several of these studies relied on separately dissolving SC and FE polymers to make blends; the hurdle of immiscibility of the main FE polymer used–PDVF, with other polymers and solvents for most SC polymers has been a major setback for this so-called FE-OPV research–in all cases, authors either utilized the Langmuir–Blodgett technique or spin-coating from solvent mixtures to make films. In most cases, these films suffered from large roughness due to phase segregation and the tendency of the FE polymer to crystallize upon thermal annealing, which is necessary to obtain the FE phase.[14]

Dr. M. Abdu-Aguye, Dr. N. Y. Doumon, Prof. L. J. A. Koster,
Prof. M. A. Loi
Photophysics and Optoelectronics
Zernike Institute for Advanced Materials
University of Groningen
Nijenborgh 4, Groningen 9747AG, The Netherlands
E-mail: l.j.a.koster@rug.nl; m.a.loi@rug.nl

Dr. N. Y. Doumon
INRS-EMT Centre for Energy
Materials and Telecommunication
1650 Boul. Lionel Boulet, Varennes, QC J3X 1S2, Canada

Dr. N. Y. Doumon
Key Laboratory of Functional Materials Physics and Chemistry
of the Ministry of Education
Jilin Normal University
Siping, Jilin 136000, China

Dr. I. Terzic, J. Dong, Dr. G. Portale, Prof. K. Loos
Macromolecular Chemistry and New Polymeric Materials
Zernike Institute for Advanced Materials
University of Groningen
Nijenborgh 4, Groningen 9747AG, The Netherlands

**ADVANCED
SCIENCE NEWS**
www.advancedsciencenews.com

**Macromolecular
Rapid Communications**
www.mrc-journal.de

On the converse side, Mehta et al., Asadi et al., and Naber et al., published studies where they attempted clarifying the role of the FE functionality in such devices. They argued that the presence of a large depolarization field in the FE which cannot be stabilized by a SC with no photogenerated carriers leads to FE compensation that cancels out the effect of poling.[15–17] In a later work, Asadi et al. rather asserted that the function of the FE polymer in the reported devices is akin to that of lithium fluoride (LiF) in fully optimized solar cells; which has been known to modify the effective work function of the aluminum cathode. Their observation was supported by the use of another fluorinated but non-FE polymer, which gave rise to similar improvement in device performance.[18]

Due to these reports showing conflicting results, and the difficulty in obtaining smooth, pinhole free films from SC-FE polymer mixtures for photovoltaic devices, the present study was designed with the goal of incorporating an A-B-A type block copolymer: P3HT-*b*-P(VDF-TrFE)-*b*-P3HT into the active layer of a P3HT:[60]PCBM solar cell (*b* represents a triazole-based linker used to couple the SC and FE blocks). By a careful selection of solvents and optimization of the deposition recipe, smooth films of both the block copolymer and the block copolymer blended with P3HT:[60]PCBM were obtained by spin coating. Structural characterizations confirm that the block copolymer films are smooth and pinhole free, which is an important requirement for device fabrication. Impedance spectroscopy experiments on fabricated parallel plate capacitors of the block copolymer yield dielectric constant values of ≈9 and 7.5 for as-cast and annealed samples, respectively–confirming the suitability of this copolymer as a high-$\varepsilon_r$ additive for OPV blends. Furthermore, we show that the photophysical properties of the copolymer agree qualitatively with previously published work on blends of FE and SC polymers[13] exhibiting quenched PL and a decrease in PL lifetime relative to the one of pristine P3HT. This is a clear indicator that the presence of electric dipoles associated with P(VDF-TrFE) affects the exciton formation and dissociation in such films. When the copolymer is incorporated in a conventional solar cell structure, it has a negative impact in terms of both PCE and photostability. We attribute this performance reduction to the variation of the nanostructure of the bulk heterojunction (BHJ) upon addition of the FE block copolymer.

**Figure 1** shows the chemical structure of the materials used in this study. In the copolymer: P3HT-*b*-P(VDF-TrFE)-*b*-P3HT, we have marked the ferroelectric component in red and the semiconducting one in blue, the triazole-based linker (*b*) is drawn in black. **Figure 2**a shows the absorbance and steady state photoluminescence (SS-PL) spectra of dilute solutions of P3HT and the copolymer in MeTHF–the almost identical spectra are an indication that the photophysical properties of the copolymer in solution are mainly dictated by P3HT; this conclusion is also supported by similar time-resolved photoluminescence measurements (TR-PL) in Figure 2b showing the PL decay lifetimes to be very similar in both cases.

As mentioned earlier, a challenge with using FE polymers in organic photovoltaics is the possibility to incorporate them into optimized BHJ blends without compromising the morphology in a manner that degrades their performance. For this reason, we first characterized thin films of the copolymer spin-coated from MeTHF, which is a good solvent for the block copolymer,



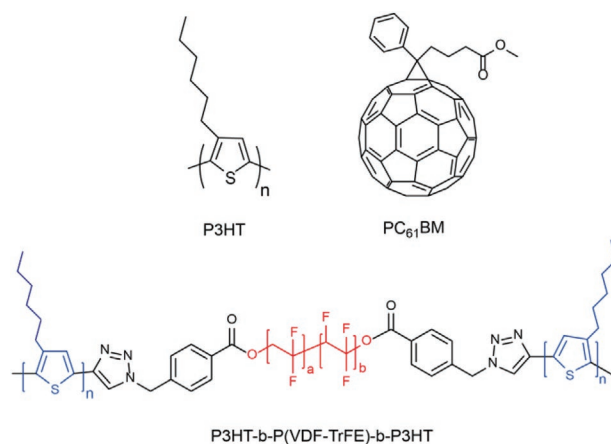**Figure 1.** Chemical structures of the materials used in this study: P3HT, [60]PCBM and the SC-FE block copolymer: P3HT-*b*-P(VDF-TrFE)-*b*-P3HT; *b* is the trizaole-based linker between the SC and FE blocks.
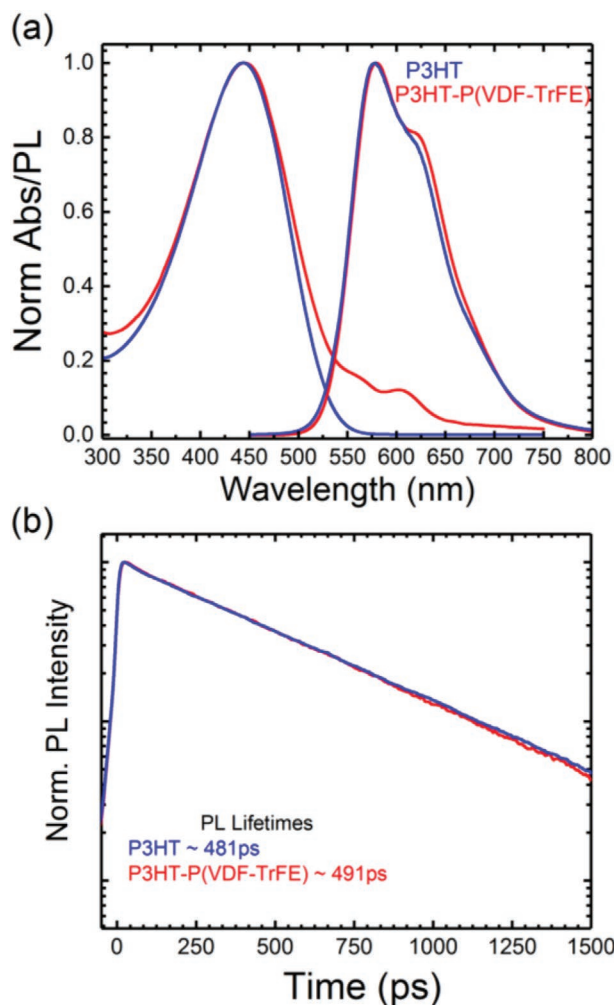


**Figure 2.** a) Normalized absorbance and steady-state photoluminescence spectra of P3HT (blue) and the P3HT-P(VDF-TrFE) (red) copolymer in MeTHF. b) Time-resolved photoluminescence spectra for the corresponding samples.
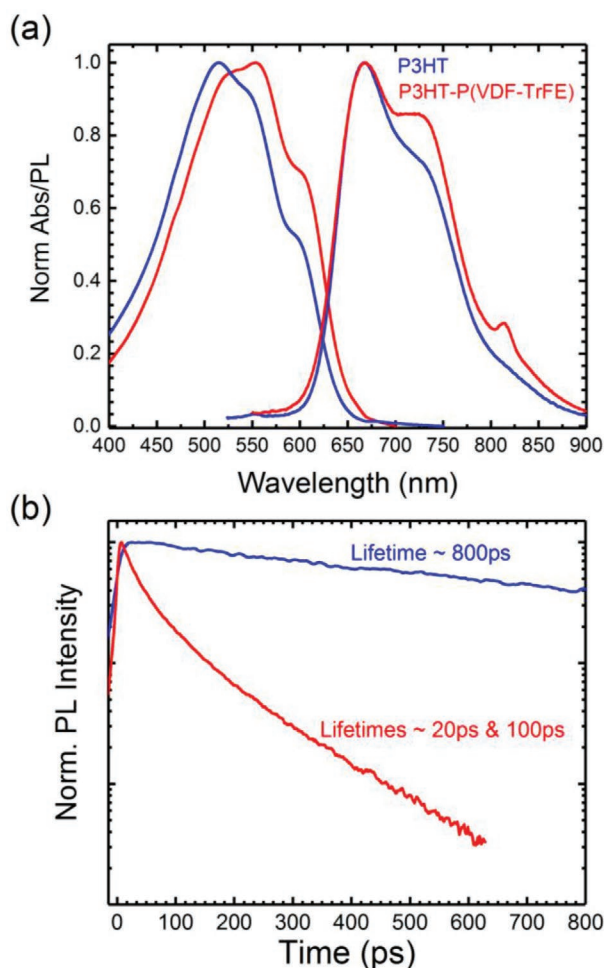
**ADVANCED
SCIENCE NEWS**
www.advancedsciencenews.com

**Macromolecular
Rapid Communications**
www.mrc-journal.de

**Figure 3.** a) Normalized absorbance and thin film PL spectra of P3HT (blue) and the P3HT-P(VDF-TrFE) (red) copolymer films. b) Time-resolved photoluminescence decays for the corresponding samples.

and also has the advantage of being a green, non-chlorinated solvent unlike those commonly used for deposition of SC polymers. The absorbance and steady-state photoluminescence measurements in **Figure 3**a show similarities between the copolymer and pristine P3HT in solid state. The red-shifted absorption of the copolymer is attributed to an increase in planarization of the P3HT chains contained within P3HT aggregates in the copolymer. This can be understood in terms of the enhanced conjugation length and the resulting decrease in the energy gap.[19,20] The different packing of the polymeric chains has also repercussions in the intensity of the vibronic features of both absorption and PL spectra. The time-resolved photoluminescence decays in Figure 3b show the most pronounced difference between the copolymer and P3HT. P3HT exhibits a mono-exponential decay with lifetime around 800 ps whereas the copolymer has a biexponential decay with lifetimes around 20 and 100 ps, respectively. This large difference in lifetimes and the appearance of an additional fast decay channel in the copolymer is evidence that in solid state, the presence of the P(VDF-TrFE) in the copolymer opens new nonradiative channels for the recombination dynamics of P3HT. Similar results were recently reported by Braz et al.[13] in blends of

fluorine-based polymers with P(VDF-TrFE) where the addition of P(VDF-TrFE) resulted in a quenched photoluminescence and in the appearance of a shorter decay lifetime.

Another important property in organic photovoltaic blends is the dielectric constant ($\varepsilon_r$). Some authors have argued that increasing the dielectric constant of the active layer blend could potentially help to improve the efficiency of organic solar cells.[21–23] There are several notable examples of polymers and fullerene derivatives with improved dielectric constants in literature which perform better than similar lower-$\varepsilon_r$ reference materials.[24–27] P(VDF-TrFE) is intrinsically a high dielectric constant material, and for this reason is often used as a polymer gate in field effect transistors owing to the high capacitance determined by the dipolar character of the C—F bonds.[28,29] To estimate the dielectric constant of the copolymer we fabricated parallel plate capacitors and we perform impedance spectroscopy. From the capacitance measurements using the expression

$$C = \varepsilon_0 \varepsilon_r \,^A/_L \tag{1}$$

where $C$ is the measured capacitance, $\varepsilon_0$ and $\varepsilon_r$ are the permittivity of free-space and the dielectric constant of the copolymer, respectively; $A$ is the area of the capacitor and $L$ is the thickness of the copolymer layer. In this manner, we obtained a value of ≈9 for the dielectric constant in as-cast films. Upon thermal annealing at 150 °C for 30 min, which is the standard treatment for P3HT solar cells; this value drops to around 7.5. The analysis of a similar work on block copolymer-based capacitors for high breakdown strength dielectrics carried out by Samant et al.[30] leads us to conclude that the $\varepsilon_r$ values we measure follow a rather simple rule-of-mixtures for the as cast copolymer, but upon thermal annealing, changes in the nanostructure may lead to phase separation which causes the decrease of the observed dielectric constant.[30] It is also important to underline that the film roughness can contribute to the imprecision of the measurement.[31]

As a further step, following the work of Nalwa et al.,[12] we aim to investigate what the effect of the FE-dipoles of P(VDF-TrFE) is on the operation of a P3HT:[60]PCBM based BHJ solar cell. To do this; we prepared the following blend solutions of P3HT:[60]PCBM in a ratio of 1:0.8 with increasing amount of the copolymer in a solvent mixture as shown in **Table 1** below.

The samples labeled "Ref" and "Ref/MeTHF" only contain P3HT and [60]PCBM but with a solvent mixture in the latter case to enable us evaluate the effect of the addition of MeTHF necessary to solubilize the block copolymer on the performance of the solar cells. Samples "5 wt%" to "20 wt%" contain increasing amounts of the copolymer relative to P3HT. In this manner, all samples are fully comparable, because they all contain the same mixture of solvents and the same total P3HT:[60]PCBM concentration (18 mg mL$^{-1}$). However, the addition of the block copolymers inserts some extra absorbing units.

According to previous studies on FE-OPV, the addition of electric dipoles in the form of P(VDF-TrFE) or similar polymers can increase the performance of solar cells by one or more of the following mechanisms: a) difference in refractive index between the copolymer and P3HT:[60]PCBM mixture can lead to scattering which may be advantageous for light absorption b) the presence of dipoles and the attendant electric field can improve dissociation of both singlet and charge transfer

**ADVANCED
SCIENCE NEWS**

www.advancedsciencenews.com

**Macromolecular
Rapid Communications**

www.mrc-journal.de

**Table 1.** Composition of the polymer blends used for the preparation of BHJ solar cells. CB = Chlorobenzene, MeTHF = 2-methyltetrahydrofuran. Total mass concentration of P3HT:[60]PCBM in all samples was 18 mg mL$^{-1}$.

| Name/Alias | Composition | Solvent |
|---|---|---|
| Ref | P3HT:[60]PCBM (1:0.8 w/w) | CB |
| Ref/MeTHF | Same as Ref | CB+MeTHF (3:1, v/v) |
| 5 wt% | Ref + 0.5 mg of copolymer | CB+MeTHF (3:1, v/v) |
| 10 wt% | Ref + 1.0 mg of copolymer | CB+MeTHF (3:1, v/v) |
| 20 wt% | Ref + 2.0 mg of copolymer | CB+MeTHF (3:1, v/v) |

**Table 2.** J–V parameters for the best performing devices. Structure: ITO/PEDOT:PSS/Active Layer/LiF/Al.

| Sample | $J_{sc}$ [A m$^{-2}$] | $V_{oc}$ [V] | FF [%] | PCE [%] |
|---|---|---|---|---|
| Ref | 98.1 | 0.57 | 68.9 | 3.83 |
| Ref/MeTHF | 93.1 | 0.56 | 67.6 | 3.54 |
| 5 wt% | 92.3 | 0.56 | 66.6 | 3.46 |
| 10 wt% | 100.1 | 0.57 | 58.3 | 3.31 |
| 20 wt% | 93.6 | 0.56 | 62.9 | 3.27 |

excitons in the devices and c) the aggregation of P(VDF-TrFE) might cause changes in the nanoscale domain sizes of P3HT and/or [60]PCBM resulting in a more favorable nano-morphology for charge transport and extraction.[11,12]

**Figure 4**a and **Table 2** show the results of the best-performing devices (structure: ITO/PEDOT:PSS/Active Layer/LiF/Al, see Figure 4b, inset) in each category (out of 16 devices for each sample). We found that the addition of MeTHF as a co-solvent (necessary for the solubilisation of the SC-FE copolymer)
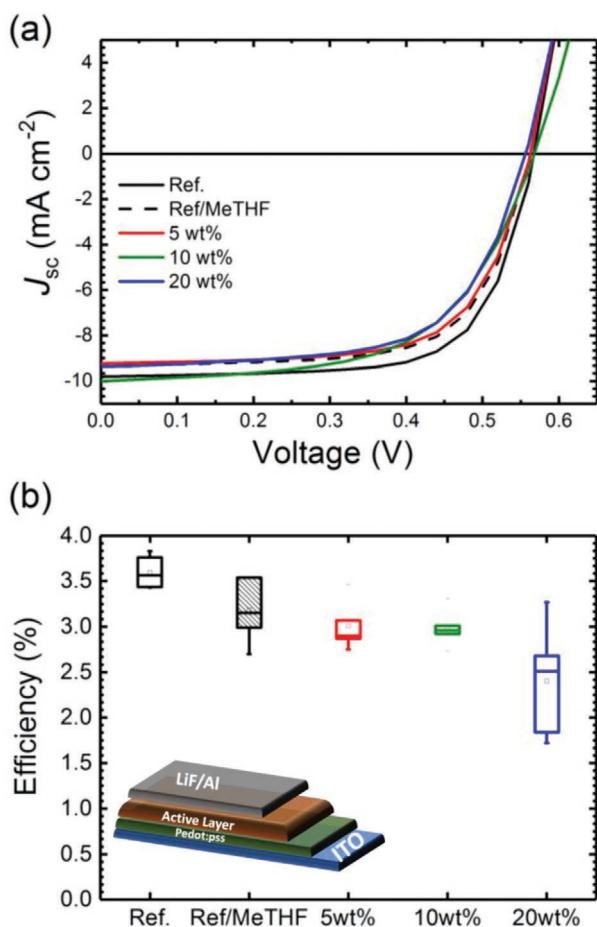
negatively impacts the PCE of the solar cells, from 3.8% to 3.5%, which is altogether not very surprising since the final nanomorphology of BHJ blends is intimately tied to the processing solvents used.[32,33] Furthermore, the addition of the SC-FE copolymer from 5% till 20% by weight also negatively affects the PCE of the solar cells, which decreases from 3.8% to 3.5%, then to 3.3%; a total of almost 15% decrease in efficiency. This variation appears as determined by a simultaneous decrease of all the partial figures of merit, namely, $J_{sc}$, $V_{oc}$ and FF. To evaluate the first two proposed mechanisms above, we measured the absorption (**Figure 5**a) and photoluminescence (Figure 5b) of the devices; the absorption should scale linearly with the measured short circuit currents and any improvement in exciton dissociation should be observable in the PL lifetime. Our results indicate that although the optical absorption is slightly improved by the addition of the copolymer, the observed short circuit current, however, decreases with increasing amounts of copolymer. In addition, both steady state and time-resolved PL (Figure S1, Supporting Information) do not show significant differences between the reference blends and copolymer-containing blends. In steady state measurements we merely observe a modulation of the intensity of the vibronic features which we believe is related to the conformation of the P3HT aggregates in the films which is affected by both the choice of solvents and the final nanomorphology.[34] This proposal is endorsed by the absence of a trend with the amount of copolymer inserted into the thin films. The recombination dynamics of polymer-fullerene blends for OPV are useful to understand relevant physical processes such as exciton diffusion, exciton separation and recombination. Time-resolved PL measurements are identical for all samples, which indicates that the samples are photophysically similar and that differences in device performance are not linked to differences in recombination mechanisms.

Atomic force microscopy (AFM) measurements on typical blends for the devices corroborate the trends in device performance. Sub-micron sized aggregates of what is probably P(VDF-TrFE) become increasingly visible going from the 5 to 20 wt% blends causing an increase of the root-mean-square roughness in 5 μm by 5 μm micrographs, from 2 nm (in the 5 wt% blend) to 7 nm (in the 20 wt% blend). Representative images of the film surface are shown in **Figure 6**a–e. It is immediately clear that in the extreme case of 20 wt%; the morphology is severely degraded, a fact that correlates with the poorer performance of the 20 wt% device. It is likely that at this amount, phase separation in the active layer occurs and the copolymer begins to aggregate thereby disrupting the active layer morphology and the transport properties.
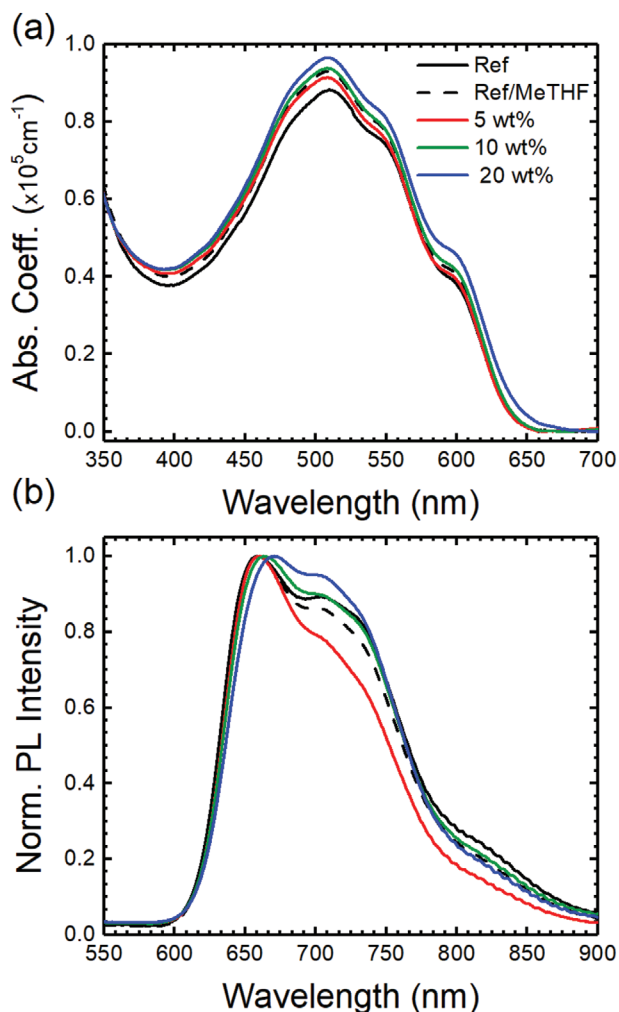


**Figure 4.** a) J–V characteristics of the best-performing devices with LiF/Al as the cathode. b) Efficiency ranges for 16 devices showing minimum, maximum, and average efficiency values; (inset) solar cell device structure.

**Figure 5.** a) Absorption and b) PL measurements for reference and copolymer-containing devices.

To gain additional information about the crystallinity, $\pi$–$\pi^*$ stacking, and the relative orientation of the polymer chains with respect to the substrate in our samples, we performed GIWAXS measurements (see Figure 6f–j). 2D GIWAXS patterns are reported as a function of the near out-of-plane $q_z$ and in-plane $q_y$ scattering vectors. The GIWAXS results reveal two important details: firstly, the use of a solvent mixture as opposed to chlorobenzene leads to a large crystallization of [60]PCBM as evidenced by the increased intensity and reduced width of the peak at 14.1 nm$^{-1}$. This indicates a high level of [60]PCBM aggregation–which is expected to have a negative influence in the hole transport properties of the active layer in agreement with the observed decrease in PCE of the reference sample cast from the solvent mixture.[35,36] Second, the signal intensity from the P3HT crystals gradually increases upon addition of the P3HT-b-P(VDF-TrFE)-b-P3HT copolymer up to 10 wt% (see Figure S4a, Supporting Information). At the same time, copolymer addition seems to promote flat-on orientation of the P3HT crystals, as shown by the scattering intensity increase in the horizontal $q_y$ direction upon copolymer addition (see Figure S4b, Supporting Information). Due to this, the fluorine atoms along
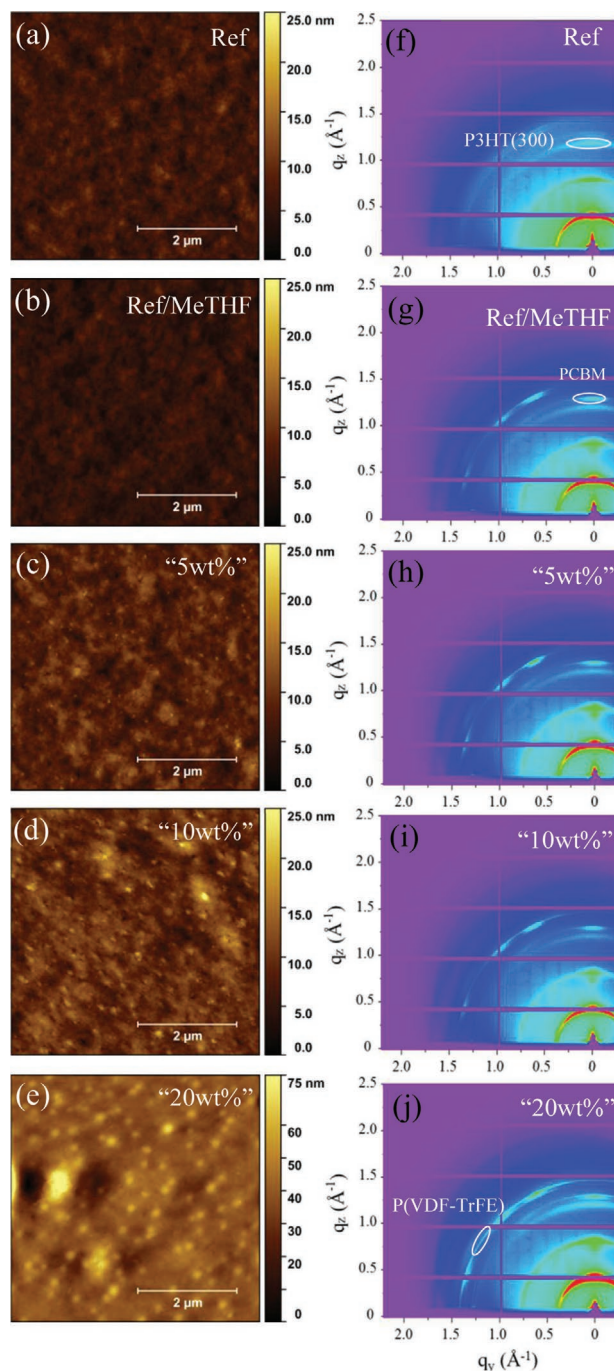


**Figure 6.** a–e) AFM micrographs and f–j) GIWAXS frames for the reference samples and copolymer-containing devices

the P(VDF-TrFE) chain are most probably not stacked vertically with respect to the substrate, which is unfavorable for dipole shifting induced by the electric field. An additional point to note is that the annealing treatment at 150 °C leads to a (re)crystallization of the copolymer from the melt state[37] ($T_m$ of P(VDF-TrFE) ≈140 °C). This results in randomly oriented P(VDF-TrFE) crystals which have a detrimental effect on the final induced internal electric field in the layer.[38,39] Increasing the copolymer concentration above 10 wt% does not improve the ordering
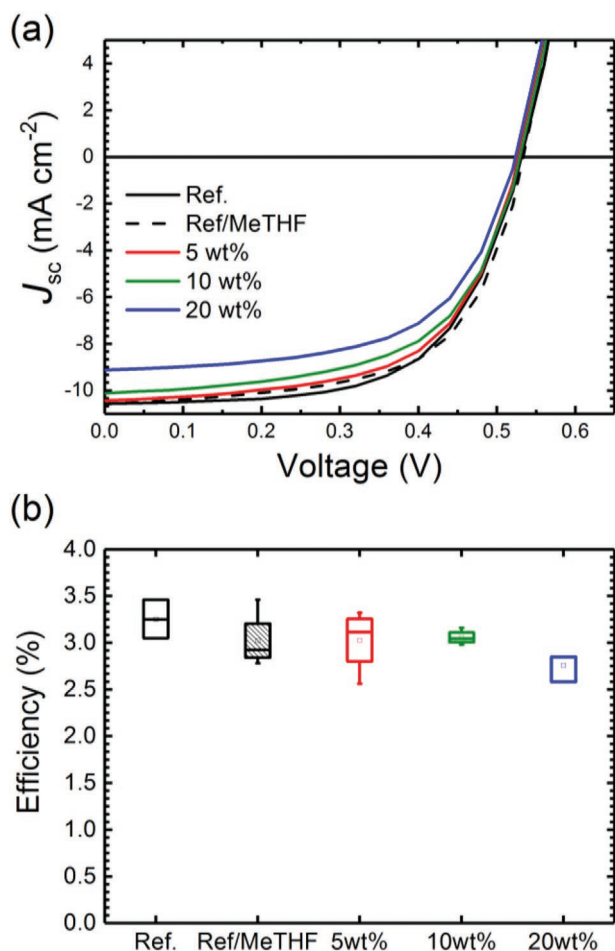
**ADVANCED
SCIENCE NEWS**

www.advancedsciencenews.com

**Macromolecular
Rapid Communications**

www.mrc-journal.de

**Figure 7.** a) J–V characteristics of the best-performing devices with only Al as cathode b) Efficiency ranges for 16 devices showing minimum, maximum and average efficiency values.

**Table 3.** J–V parameters for the best performing devices without LiF. Structure: ITO/PEDOT:PSS/Active Layer/Al.

| Device | $J_{sc}$ [A m$^{-2}$] | $V_{oc}$ [V] | FF [%] | PCE [%] |
|---|---|---|---|---|
| Ref | 105.7 | 0.53 | 61.6 | 3.46 |
| Ref/MeTHF | 105.7 | 0.53 | 61.4 | 3.43 |
| 5 wt% | 104.4 | 0.53 | 60.4 | 3.32 |
| 10 wt% | 101.2 | 0.53 | 58.9 | 3.16 |
| 20 wt% | 91.3 | 0.52 | 59.7 | 2.85 |

(see **Table 3**). Interestingly, the copolymer containing devices are less affected by the absence of LiF compared to the reference devices and give a lower scatter in PCE values across multiple sets of devices, implying that cathode modification likely occurs as they proposed. We further note that these devices without the LiF interlayer were more prone to degradation–likely due to interactions between the active layer and the Al electrode.

While the above sections demonstrate the difficulty in using FE polymers to improve OPV performance; many unanswered questions remain regarding the role of the FE polymers in OPV active-layer blends. Such questions are related to a) the charge (especially hole) mobilities may be affected adversely in blends containing FE polymers because of the disrupted P3HT crystallization b) the effect of the added FE copolymer on stability of the devices and finally c) the influence of the ferroelectricity of the copolymer on the solar cell device performance. To answer some of these questions we carried out light intensity dependent measurements, poling measurements and also light-induced degradation on devices containing the block copolymer. Our light dependent $V_{oc}$ and $J_{sc}$ measurements reveal no significant differences in recombination mechanisms between samples, with both the ideality factor (n) and α exponent falling within very similar ranges (see Figure S2a,b, Supporting Information).

To check the effect of the ferroelectricity of the copolymer on the performance of the solar cells, we performed poling experiments like those reported in earlier studies. In theory, applying an electric field greater than or equal to the coercive field of the FE polymer to the active layer of the solar cell should switch the dipoles of the FE to align with the electric field. This experiment was performed by applying a voltage pulse to the electrodes of the solar cell. The copolymer has a coercive field around 80 V μm$^{-1}$ (see Figure S5, Supporting Information), while values for dipole reorientation times for P(VDF-TrFE) from the literature[40] suggest that pulses of the order of 1 ms are sufficient to switch them.

Using a semiconductor parameter analyzer, voltage pulses of varying magnitudes (5–20 V), durations (10 ms–1 s), and polarities were applied to the devices while monitoring the voltage across with an oscilloscope to ensure that the devices reached the set voltage. In all cases, the devices performed exactly the same before and after poling regardless of magnitude, duration, and polarity of the pulse. We believe these findings are definitive proof of assertions by Asadi and Naber[16–18] that ferroelectric compensation cancels out the effect of poling and renders the strategy of adding FE polymers to OPV blends inoperative.

Furthermore, since P(VDF-TrFE) is by itself a rather inert polymer under ambient conditions, we examined the

further, as a global drop of the scattered intensity is registered with respect to the 10 wt% sample (see Figure S4a, Supporting Information). This is in line with the morphology degradation observed by AFM for the 20 wt% sample in Figure 6e.

At this point, we can conclude that the addition of the FE copolymer does not improve the performance of the active layer and most of the phenomena reported earlier as possible cause(s) of improvement do not occur in our blends.

To further understand the lower device performance in the copolymer containing samples, we sought to elucidate the role of LiF in fully optimized devices. Asadi et al.[18] had proposed that adding fluorinated (co)polymers as interlayers to P3HT:[60] PCBM blends only results in improvement via modification of the cathode interface, i.e., the copolymer plays the role of LiF in a fully optimized solar cell. If this was indeed the case, we hypothesized that the devices containing copolymer would be less affected by the absence of LiF than the reference devices. Results from devices fabricated in the same manner as explained earlier but without LiF are shown in **Figure 7**a, confirming our previous observation that addition of copolymer impedes the performance of solar cells. Also, the absence of LiF causes a slight reduction in the efficiency of the devices by ≈5% to 13%

UV-photostability of the copolymer containing devices versus the reference devices similarly as fully described earlier in work by Doumon et al.[41] Results obtained from these measurements indicate that adding the copolymer to the active layer decreases the UV photostability of the devices. The copolymer-containing devices lose between 6–10% of their PCE during illumination (see Figure S3, Supporting Information) mainly due to losses in $J_{sc}$ and small losses in FF; while the reference devices recorded about 3–4% loss in initial PCE over the same period. While the reasons for this observation are not immediately clear, we speculate that there might be some UV-induced photodegradation of the triazole linker contained in the copolymer.[42] These notable losses could also be linked to the deterioration of the active layer containing the copolymer as shown by AFM images. Further investigation of this observation is, however, outside the scope of this paper.

We have demonstrated that A-B-A copolymers where A is a conjugated polymer and B is a ferroelectric polymer can be blended with organic semiconductors to obtain good quality thin films. The block copolymer P3HT-*b*-P(VDF-TrFE)-*b*-P3HT has been successfully incorporated into the active layer of a P3HT:[60]PCBM solar cell. Our results indicate that the addition of the block copolymer impedes the performance of optimized solar cells, most probably because of the disruption of the nanomorphology of the bulk heterojunction. Furthermore, we demonstrate that the addition of FE components into OPV blends present additional challenges such as decreased photostability. Our work highlights the importance of thorough investigation into other potential effects of additives for organic solar cells, most notably in cases where the additive has a large influence in the nanostructure of the blend.

## Experimental Section

*Materials*: Highly regioregular electronic grade Poly(3-hexylthiophene) and PCBM were obtained from Rieke Metals and Solenne B.V., respectively, and used without further purification. The anhydrous solvents: 2-Methltetrahydrofuran (MeTHF ≥ 99%, inhibitor free) and Chlorobenzene (99.8%) were purchased from Sigma Aldrich.

The P3HT-*b*-P(VDF-TrFE)-*b*-P3HT triblock copolymer was synthesized using copper catalyzed [3 + 2] Huisgen azide/alkyne cycloaddition of alkyne terminated P3HT and azide terminated P(VDF-TrFE). Highly regioregular, low polydisperse P3HT was prepared via Grignard metathesis polymerization, as previously described in the literature.[43] In addition, a free radical polymerization starting from a chlorine functionalized benzoyl peroxide as initiator was used to prepare chlorine terminated P(VDF-TrFE).[44] Subsequent treatment of the polymer with sodium azide yielded the complete replacement of chlorine with azide end groups. Finally, the coupling reaction was performed in THF where a 1.3-fold excess of P3HT was used compared to P(VDF-TrFE) to ensure a complete reaction. Afterward, the polymer solution was passed through neutral alumina to remove the metal catalyst, while excess P3HT was removed by washing with chloroform to obtain the pure triblock copolymer. Further information on the synthesis can be found in ref. [46].

*Thin-Film Preparation*: Thin-films of the copolymer were spin-coated from warm solutions of the copolymer in 2-Methyltetrahydrofuran (MeTHF) onto preheated glass substrates in a Nitrogen-filled flow box at a speed of 600 rpm for 5 s and spin dried for 120 s.

Bulk heterojunction solar cells were similarly fabricated on ITO-coated glass substrates, which were cleaned sequentially in soap, water, acetone and isopropanol. The cleaned ITO-glass substrates were dried, annealed at 140 °C for about 10 min and treated with UV–ozone

for about 20 min. PEDOT:PSS (Klavios) was spin-coated at a speed of 1500 rpm for 60 s to give ≈50 nm thick layers. The films were then dried in an oven and transferred to a Nitrogen-filled flow box. The active layers were spin-coated from heated blend solutions at a speed of 600 rpm for 5 s and spin dried at 120 s. The substrates were then transferred into an evaporator and kept in vacuum overnight, with the chamber kept at least at $10^{-7}$ mbar. The devices were completed by evaporation of LiF (1 nm)/ Al (100 nm) or bare-Al (100 nm). Finally, the full devices were annealed at 150 °C for 30 min before characterization.

*Absorption Spectroscopy*: Absorbance measurements were carried out on dilute solutions of P3HT and P3HT-P(VDF-TrFE) in 2 mm path length quartz cuvettes and on masked areas of spin-coated thin films on glass. The instrument used was a dual-beam Shimadzu UV–vis–NIR spectrophotometer (UV–VIS–NIR-3600)

*Steady State and Time Resolved Photoluminescence (PL) Spectroscopy*: Steady state photoluminescence measurements were carried out by exciting the samples with the second harmonic (≈400 nm) of a mode locked Ti-Sapphire laser (Mira 900, Coherent) delivering 150 fs pulses at a repetition rate of 76 MHz. The excitation beam was spatially limited by an iris and focused onto a spot of ≈100 µm by a 150 mm focal length lens while the power was adjusted using neutral density filters. Steady state spectra were collected by a spectrograph with a grating of 30 lines/ mm and further recorded by a Hamamatsu em-CCD camera.

The same pulsed excitation was used for time-resolved measurements but photoluminescence decays were instead collected with a Hamamatsu streak camera unit working in Synchroscan mode (time resolution ≈2 ps) with a cathode sensitive in the visible region.

All spectra were corrected for the response of the instrument using a calibrated lamp.

*Atomic Force Microscopy (AFM)*: Measurements of surface morphology were performed on a Bruker Multimode MMAFM-2 in ScanAsyst mode on spin-coated samples on glass; or on blends spin-coated on PEDOT:PSS in the case of working devices.

*Grazing Incidence Wide-Angle X-Ray Scattering (GIWAXS)*: GIWAXS measurements were performed at the Dutch-Belgian beamline (DUBBLE) BM26B at the European Synchrotron Radiation Facility (ESRF), Grenoble, France.[45] An X-ray beam with energy of 12 keV ($\lambda$ = 1.033 Å) was used with a sample-to-detector distance of 410 mm. 2D GIWAXS patterns were collected using a Pilatus 1M solid state silicon X-ray detector and using an exposure time of 60 s per frame. The beam center coordinates on the detector image, the sample-to-detector distance and the probed scattering angle range were calibrated using the known position of diffracted rings from standard Silver behenate and $\alpha$-Al$_2$O$_3$ powders. An incident angle of 0.15° was used for all the measurements. The GIWAXS patterns are presented as a function of the near out-of-plane $q_z$ and in-plane $q_y$ scattering vectors, according to their standard definition.

*Solar Cell Characterization*: The completed and annealed devices were transferred into a measurement glovebox, in an inert environment with H$_2$O and O$_2$ levels kept at <0.1 ppm. The current–voltage ($J$–$V$) measurements were performed with a Steuernaugel solar constant 1200 metal halide lamp with an AM1.5G white light spectrum calibrated to 1 sun by a silicon reference cell.

For the degradation experiment, devices kept at room temperature by active cooling, were continuously exposed to light at open circuit condition and the $J$–$V$ parameters were taken at 5 min intervals for 120 min for each sample. For light dependent measurements, a series of filters were coupled with a long-pass filter to vary the light intensity from around 1 to 1000 W m$^{-2}$ under the same conditions.

*Impedance Spectroscopy*: Parallel plate capacitors were fabricated from thin films of the copolymer and completed by the evaporation of aluminum (Al) electrodes, for obtaining a structure glass/ITO/ PEDOT:PSS (≈50 nm)/Pristine copolymer/Al (100 nm). Measurements were performed in the frequency range 10–10$^6$ Hz with an AC drive voltage of 10 mV and no applied DC bias. The capacitance was obtained in a frequency range of 100 to 10$^5$ Hz from the fitting of the RC equivalent circuit and the dielectric constant was calculated using Equation (1). The capacitance is averaged over different device areas.

## Supporting Information

## Acknowledgements

## Conflict of Interest

The authors declare no conflict of interest.

## Keywords

[1] F. Goubard, G. Wantz, *Polym. Int.* **2014**, *63*, 1362.
[2] P. P. Khlyabich, B. Burkhart, B. C. Thompson, *J. Am. Chem. Soc.* **2011**, *133*, 14534.
[3] L. Lu, W. Chen, T. Xu, L. Yu, *Nat. Commun.* **2015**, *6*, 7327.
[4] J.-W. Lee, D.-Y. Son, T. K. Ahn, H.-W. Shin, I. Y. Kim, S.-J. Hwang, M. J. Ko, S. Sul, H. Han, N.-G. Park, *Sci. Rep.* **2013**, *3*, 1050.
[5] H. Fu, S.-W. Tsang, Y. Zhang, J. Ouyang, J. Lu, K. Yu, Y. Tao, *Chem. Mater.* **2011**, *23*, 1805.
[6] J. H. Rhee, C.-C. Chung, E. W.-G. Diau, *NPG Asia Mater.* **2013**, *5*, 68.
[7] J. Tang, L. Brzozowski, D. A. R. Barkhouse, X. Wang, R. Debnath, R. Wolowiec, E. Palmiano, L. Levina, A. G. Pattantyus-Abraham, D. Jamakosmanovic, E. H. Sargent, *ACS Nano* **2010**, *4*, 869.
[8] Y. Shi, F. Li, Y. Chen, *New J. Chem.* **2013**, *37*, 236.
[9] S. Liu, D. Chen, W. Zhou, Z. Yu, L. Chen, F. Liu, Y. Chen, *Macromolecules* **2019**, *52*, 4359.
[10] J. B. Kim, K. Allen, S. J. Oh, S. Lee, M. F. Toney, Y. S. Kim, C. R. Kagan, C. Nuckolls, Y.-L. Loo, *Chem. Mater.* **2010**, *22*, 5762.
[11] Y. Yuan, T. J. Reece, P. Sharma, S. Poddar, S. Ducharme, A. Gruverman, Y. Yang, J. Huang, *Nat. Mater.* **2011**, *10*, 296.
[12] K. S. Nalwa, J. A. Carr, R. C. Mahadevapuram, H. K. Kodali, S. Bose, Y. Chen, J. W. Petrich, B. Ganapathysubramanian, S. Chaudhary, *Energy Environ. Sci.* **2012**, *5*, 7042.
[13] T. Braz, A. L. Mendonça, R. E. Di Paolo, J. Morgado, *J. Lumin.* **2016**, *178*, 457.
[14] P. Martins, A. C. Lopes, S. Lanceros-Mendez, *Prog. Polym. Sci.* **2014**, *39*, 683.
[15] R. R. Mehta, B. D. Silverman, J. T. Jacobs, *J. Appl. Phys.* **1973**, *44*, 3379.
[16] K. Asadi, D. M. De Leeuw, B. De Boer, P. W. M. Blom, *Nat. Mater.* **2008**, *7*, 547.
[17] R. C. G. Naber, J. Massolt, M. Spijkman, K. Asadi, P. W. M. Blom, D. M. De Leeuw, *Appl. Phys. Lett.* **2007**, *90*, 113509.
[18] K. Asadi, P. De Bruyn, P. W. M. Blom, D. M. De Leeuw, *Appl. Phys. Lett.* **2011**, *98*, 183301.
[19] F. C. Spano, *Chem. Phys.* **2006**, *325*, 22.
[20] J. D. Roehling, I. Arslan, A. J. Moul, *J. Mater. Chem.* **2012**, *22*, 2498.
[21] L. J. A. Koster, S. E. Shaheen, J. C. Hummelen, *Adv. Energy Mater.* **2012**, *2*, 1246.
[22] S. Torabi, F. Jahani, I. Van Severen, C. Kanimozhi, S. Patil, R. W. a. Havenith, R. C. Chiechi, L. Lutsen, D. J. M. Vanderzande, T. J. Cleij, J. C. Hummelen, L. J. A. Koster, *Adv. Funct. Mater.* **2015**, *25*, 150.
[23] H. J. Son, B. Carsten, I. H. Jung, L. Yu, *Energy Environ. Sci.* **2012**, *5*, 8158.
[24] S. Zhang, Z. Zhang, J. Liu, L. Wang, *Adv. Funct. Mater.* **2016**, *26*, 6107.
[25] F. Jahani, S. Torabi, R. C. Chiechi, L. J. A. Koster, J. C. Hummelen, L. Jan, A. Koster, J. C. Hummelen, *Chem. Commun.* **2014**, *50*, 10645.
[26] M. Breselge, I. Van Severen, L. Lutsen, P. Adriaensens, J. Manca, D. Vanderzande, T. Cleij, *Thin Solid Films* **2006**, *511-512*, 328.
[27] X. Chen, Z. Zhang, Z. Ding, J. Liu, L. Wang, *Angew. Chem., Int. Ed.* **2016**, *55*, 10376.
[28] M. S. Lu, H. C. Wu, Y. W. Lin, M. Ueda, W. C. Chen, *React. Funct. Polym.* **2016**, *108*, 39.
[29] S. W. Jung, J. K. Lee, Y. S. Kim, S. M. Yoon, I. K. You, B. G. Yu, Y. Y. Noh, *Curr. Appl. Phys.* **2010**, *10*, 58.
[30] S. P. Samant, C. A. Grabowski, K. Kisslinger, K. G. Yager, G. Yuan, S. K. Satija, M. F. Durstock, D. Raghavan, A. Karim, *ACS Appl. Mater. Interfaces* **2016**, *8*, 7966.
[31] G. Palasantzas, J. Barnaś, *Phys. Rev. B* **1997**, *56*, 7726.
[32] W. Cao, J. Xue, *Energy Environ. Sci.* **2014**, *7*, 2123.
[33] S. Kouijzer, J. J. Michels, M. van den Berg, V. S. Gevaerts, M. Turbiez, M. M. Wienk, R. A. J. Janssen, M. Van Den Berg, S. Gevaerts, *J. Am. Chem. Soc.* **2013**, *135*, 12057.
[34] J. Clark, C. Silva, R. H. Friend, F. C. Spano, *Phys. Rev. Lett.* **2007**, *98*, 206406.
[35] M. Shao, J. Keum, J. Chen, Y. He, W. Chen, J. F. Browning, J. Jakowski, B. G. Sumpter, I. N. Ivanov, Y. Z. Ma, C. M. Rouleau, S. C. Smith, D. B. Geohegan, K. Hong, K. Xiao, *Nat. Commun.* **2014**, *5*, 1.
[36] X. Yang, J. Loos, S. C. Veenstra, W. J. H. Verhees, M. M. Wienk, J. M. Kroon, M. A. J. Michels, R. A. J. Janssen, *Nano Lett.* **2005**, *5*, 579.
[37] N. Meng, X. Zhu, R. Mao, M. J. Reece, E. Bilotti, *J. Mater. Chem. C* **2017**, *5*, 3296.
[38] J. S. Lee, A. A. Prabu, K. J. Kim, *Polymer* **2010**, *51*, 6319.
[39] Y. Wu, X. Li, Y. Weng, Z. Hu, A. M. Jonas, *Polymer* **2014**, *55*, 970.
[40] D. Mao, B. E. Gnade, M. A. Quevedo-Lopez, in *Ferro-electrics - Physical Effects*, IntechOpen, London **2011**, https://doi.org/10.5772/17147.
[41] N. Y. Doumon, G. Wang, R. C. Chiechi, L. Jan, A. Koster, *J. Mater. Chem. C* **2017**, *5*, 6611.
[42] E. M. Burgess, R. Carithers, L. McCullagh, *J. Am. Chem. Soc.* **1968**, *90*, 1923.
[43] M. Jeffries-El, G. Sauvé, R. D. Mccullough, *Macromolecules* **2005**, *38*, 10346.
[44] V. S. D. Voet, G. O. R. Alberda Van Ekenstein, N. L. Meereboer, A. H. Hofman, G. Ten Brinke, K. Loos, *Polym. Chem.* **2014**, *5*, 2155.
[45] W. Bras, I. P. Dolbnya, D. Detollenaere, R. Van Tol, M. Malfois, G. N. Greaves, A. J. Ryan, E. Heeley, *J. Appl. Crystallogr.* **2003**, *36*, 791.
[46] V. Voet, *Ph.D. Thesis*, University of Groningen, **2015**.